International Flame Research Foundation
The Finnish and Swedish National Committees
Finnish – Swedish Flame Days 2013

Modeling of sulfation of potassium chloride by ferric sulfate addition during grate-firing of biomass

Hao Wu*[A], Jacob Boll Jespersen[A], Martti Aho[B], Kari Paakkinen[B], Raili Taipale[B], Flemming Jappe Frandsen[A], Peter Glarborg[A]

A) Department of Chemical and Biochemical Engineering, Technical University of Denmark, DK-2800 Kgs. Lyngby, Denmark

B) VTT Technical Research Centre of Finland, P.O. Box 1603, FI-40101, Jyväskylä, Finland

* Corresponding author, haw@kt.dtu.dk

ABSTRACT

Potassium chloride, KCl, formed from critical ash-forming elements released during combustion may lead to severe ash deposition and corrosion problems in biomass-fired boilers. Ferric sulfate, $Fe_2(SO_4)_3$ is an effective additive, which produces sulfur oxides (SO_2 and SO_3) to convert KCl to the less harmful K_2SO_4. In the present study the decomposition of ferric sulfate is studied in a fast-heating rate thermogravimetric analyzer (TGA), and a kinetic model is proposed to describe the decomposition process. The yields of SO_2 and SO_3 from ferric sulfate decomposition are investigated in a laboratory-scale tube reactor. It is revealed that approximately 40% of the sulfur is released as SO_3, the remaining fraction being released as SO_2. The proposed decomposition model of ferric sulfate is combined with a detailed gas phase kinetic model of KCl sulfation, and a simplified model of K_2SO_4 condensation in order to simulate the sulfation of KCl by ferric sulfate addition during grate-firing of biomass. The simulation results show good agreements with the experimental data obtained in a pilot-scale biomass grate-firing reactor, where different amounts of ferric sulfate was injected on the grate or into the freeboard. In addition, the simulations of elemental sulfur addition on the grate fit well with the experimental data. The results suggest that the SO_3 released from ferric sulfate decomposition is the main contributor to KCl sulfation, and that the effectiveness of the ferric sulfate addition is sensitive to actual temperature in the system. When the ferric sulfate is injected on the grate, the majority of the released SO_3 is rapidly converted to SO_2 due to the high temperatures, resulting in a low effectiveness similar to that of elementary sulfur addition on the grate. On the other hand, when the ferric sulfate is injected into the freeboard where the temperatures are below 1050^{o}C, the majority of the released SO_3 contributes to the formation of K_2SO_4, leading to a high effectiveness in KCl destruction. Overall, the model developed in this work facilitates an optimal use of ferric sulfate in biomass combustion.

Keywords: Biomass combustion; Sulfate additive; Chemical kinetics modeling

1 Introduction

Alkali chlorides released during biomass combustion may lead to severe ash deposition and corrosion problems in boilers. A feasible method to mitigate these alkali chlorides-induced problems, is to use additives to convert the alkali chlorides to less harmful alkali species, and release the chlorine e.g. as HCl. Sulfur-based additives, such as elemental sulfur [1,2], SO_2 [2-5], ammonium sulfate [2,6-10], aluminum sulfate and ferric sulfate [5,11], have been tested in biomass combustion systems through years. Thermal decomposition or oxidation of these additives produces SO_2 and SO_3, which convert corrosive alkali chlorides to alkali sulfates and HCl through the following global reaction:

$$2MCl + SO_2 + 0.5O_2 + H_2O \longrightarrow M_2SO_4 + 2HCl \quad (1)$$

where M is K or Na.

The effectiveness of different sulfur-based additives has been compared experimentally [1,2,4,11]. Sulfates (e.g. ammonium sulfate, aluminum sulfate and ferric sulfate) are in general much more effective, than elemental sulfur or SO_2 [1,2,11]. In a biomass-fired boiler where the gas residence time is typically very short (a few seconds), SO_3 is needed in order to achieve a fast sulfation of alkali chlorides [12]. However, the homogeneous oxidation of SO_2 to SO_3 is usually limited in the boiler because the reaction is thermodynamically restricted at high temperatures (e.g.>1100^{o}C), and is kinetically limited at low temperatures (e.g.<900^{o}C) [13,14]. Therefore, with the addition of SO_2 or elemental sulfur, only a small fraction would be oxidized to SO_3 and contribute to the sulfation reaction [1]. On the other hand, the thermal decomposition of sulfate additives is believed to produce SO_3 directly, resulting in a fast sulfation of alkali chlorides [1,11].

In spite of the extensive experimental studies on the utilization of sulfate additives [1,2,7,8,10,11,15], investigations on the decomposition rates and products of these additives are scarce. In relation to this, no modeling work has been carried out to simultaneously simulate the decomposition of the sulfate additives, and the sulfation of KCl under biomass-fired boiler conditions. The development of such a model would facilitate the optimization of sulfate additive utilization during biomass combustion.

The objective of this study was to develop a model for the sulfation of KCl by $Fe_2(SO_4)_3$-addition during biomass combustion. The decomposition of ferric sulfate was investigated in a high-heating rate thermogravimetric analyzer (TGA), and in a laboratory-scale tube reactor in order to understand the decomposition kinetics and the product distribution. The model developed combines a volumetric reaction model for $Fe_2(SO_4)_3$-decomposition with a detailed gas-phase kinetic model for sulfation of KCl [13], and a simplified model for homogeneous and heterogeneous condensation of K_2SO_4 [16]. The model was validated by comparison with experimental results from biomass combustion on a pilot-scale grate combustor, where $Fe_2(SO_4)_3$ was injected in different amounts on the grate or into the freeboard [5].

2 Experimental Procedure

2.1 Fast heating rate TGA

Decomposition of ferric sulfate, $Fe_2(SO_4)_3$, was studied in a fast heating rate Netzsch STA 449 F1 Jupiter thermogravimetric analyzer (TGA). The experiments were carried out under N_2 environment, using a ferric sulfate hydrate ($Fe_2(SO_4)_3 \cdot xH_2O$) with a purity of 97% from Sigma-Aldrich. In the experiments the sample was first dehydrated by heating up to 250°C at a rate of 10°C/min. After 30 minutes holding time, the sample was heated at a rate of 500°C/min to an end temperature, which was varied from 600°C to 800°C in steps of 50°C. The sample was held at the end temperature until a full-conversion was achieved.

2.2 Laboratory-scale tube reactor

Experiments were conducted in a laboratory-scale tube reactor to identify the yield of SO_2 and SO_3 from the decomposition of Fe2(SO4)3. The experiments were carried out under well-controlled temperature and flow conditions, and the SO_2 released were analyzed continuously by an IR-based Fischer-Rosemount NGA 2000 analyzer. Based on the measured SO_2 concentration over time, a fractional conversion of the S in $Fe_2(SO_4)_3$ to SO_2 was calculated. The remaining S is assumed to be released as SO_3. The temperature range studied was 600–1000°, where homogeneous decomposition of SO_3 to SO_2 is expected to be negligible.

2.3 Pilot-scale grate-firing reactor

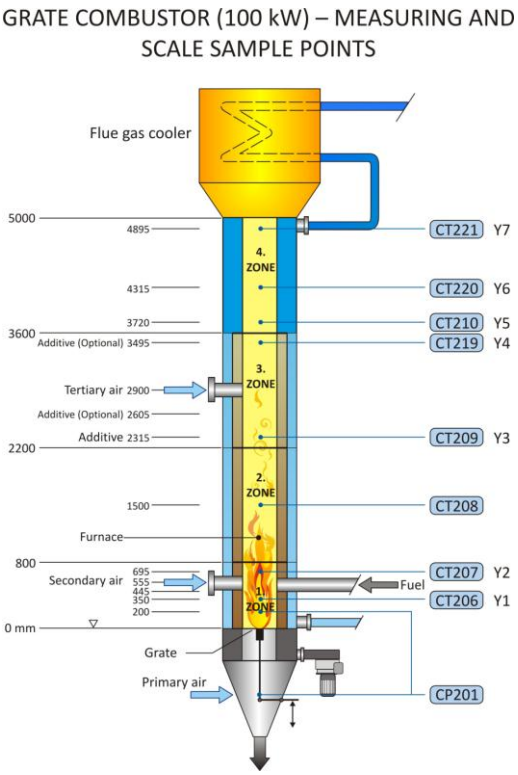

Figure 1 A schematic diagram of the 100 kW grate combustor at VTT Technical Research Centre of Finland [17].

A series of experiments has been carried out in a 100 kW grate combustor located at the VTT Technical Research Centre of Finland in order to study the effect of $Fe_2(SO_4)_3$ addition on KCl-destruction during grate-firing of biomass [5]. The data from the experimental campaign are used for model validation in this work. A schematic diagram of the grate combustor is shown in Figure 1.

Table 1 . Fuel analysis of a mixture of 60% wood chips and 40% corn stover (the oxygen content is obtained by difference).

Analysis	Unit	Value
Moisture	wt.%	29
LHV (as received)	MJ/kg	10.7
Ash	wt.% dry	8.0
S	wt.% dry	0.04
Cl	wt.% dry	0.305
C	wt.% dry	45.42
H	wt.% dry	5.69
N	wt.% dry	0.32
K	wt.% dry	0.83
O	wt.% dry	39.40

During the experiments, the combustion of the biomass took place on a rotating grate equipped with narrow primary air inlets, and the secondary air was injected above the grate to facilitate complete combustion. The fuel used in the experiments was a mixture of Spanish wood chips and 40±4% (energy basis) corn stover, with compositions as shown in Table 1. The experiments were conducted at a constant fuel load of 89±5 kW which secured the temperature versus residence time profiles in the freeboard being representative of a grate-fired power plant [5]. The temperatures in the freeboard were measured by a suction pyrometer at different sampling ports. At port Y5, an impactor was used to sample the alkali vapors and the small particulates generated from combustion. The chemical composition of the collected aerosols was analyzed by atomic absorption spectrometry (AAS) and ion chromatography (IC). The flue gas was analyzed by traditional on-line analyzers for O_2, CO and CO_2 after the cyclone placed downstream of the flue gas cooler. In addition, a flue gas flow was sampled at port Y7 to measure HCl and SO_2 through a FTIR analyzer. For the experiments with $Fe_2(SO_4)_3$ addition via port Y3, an aqueous solution of $Fe_2(SO_4)_3$ was sprayed into the furnace with an average droplet size of ~12 µm. During some experiments, solid $Fe_2(SO_4)_3$ and elemental sulfur were added to the grate. The dosage of sulfur additives, determined as the molar ratio of $S_{reagent}/Cl_{fuel}$, was varied in the experiments.

3 Model development and simulation

The model developed in this work involves a description of $Fe_2(SO_4)_3$ decomposition, a detailed reaction mechanism for the gas-phase reactions of SO_2/SO_3 and KCl [13], and a simplified model for homogeneous condensation of K_2SO_4 [16].

The decomposition of $Fe_2(SO_4)_3$ is assumed to be kinetically controlled and follow the volumetric reaction model:

$$\frac{dW}{dt} = -kW \tag{2}$$

where W is the relative mass of the anhydrous ferric sulfate defined as:

$$W = \frac{m - m_\infty}{m_0 - m_\infty} \tag{3}$$

where m_0 (g) is the mass of the anhydrous $Fe_2(SO_4)_3$ before decomposition, m_∞ (g) is the mass of the residue after decomposition, and m (g) is the mass of anhydrous ferric sulfate at t (s) during decomposition.

The rate constant k in Eq. 2 is assumed to follow an Arrhenius expression:

$$k = A \cdot \exp(-\frac{E}{RT}) \tag{4}$$

where A (s^{-1}) is the pre-exponential factor, E (kJ/mol) the activation energy, R (kJ/mol/K) the gas constant, and T(K) the temperature of the particle. The activation energy (E) and the pre-exponential factor (A) in Eq. 4 are derived from the TGA experiments. As shown in Figure 2a, during the isothermal periods of the fast-heating rate TGA experiments, a high linearity is seen between ln(k) and 1/T, indicating that Eq. 4 can satisfactorily describe the decomposition of ferric sulfate. The activation energy (E) and the pre-exponential factor (A) derived from Figure 2a are 236.8 (kJ/mol) and $1.079*10^{11}$ (s^{-1}), respectively.

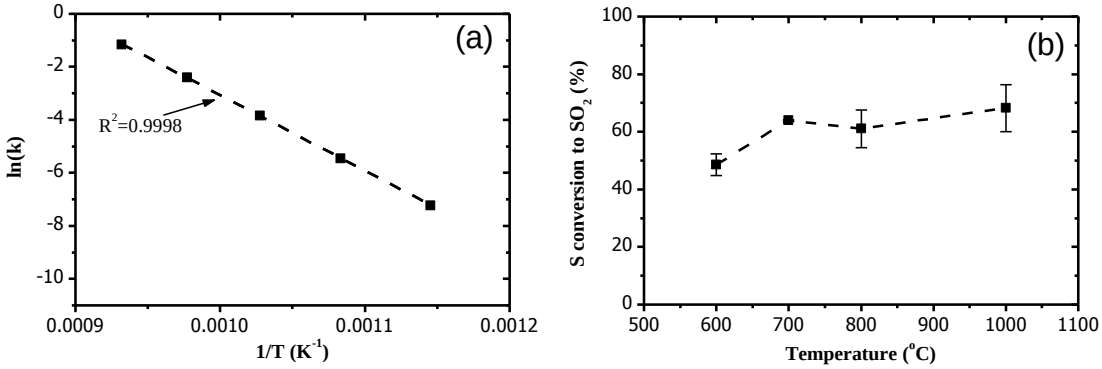

Figure 2 (a) Correlation between ln(k) and 1/T during ferric sulfate decomposition in isothermal periods of the fast-heating rate TGA experiments (b) the percentage of sulfur in ferric sulphate converted to SO_2 (%) at different temperatures in a nitrogen environment.

Figure 2b shows the results from the laboratory-scale tube reactor experiments. It can be seen that in the temperature range of 700–1000°C, approximately 60% of the S in $Fe_2(SO_4)_3$ is released as SO_2. Since the decomposition of $Fe_2(SO_4)_3$ upon injection in a furnace primarily occurs at temperatures above 700°C, it is reasonable to assume for modeling purposes that 60% of the S from $Fe_2(SO_4)_3$ decomposition is released as SO_2, whereas the remaining 40% is released as SO_3. Based on this assumption, we propose the following global reaction for the decomposition of ferric sulfate:

$$Fe_2(SO_4)_3 \longrightarrow Fe_2O_3 + 1.2SO_3 + 1.8SO_2 + 0.9O_2 \tag{5}$$

In order to describe the gas phase reactions between KCl and SO_2/SO_3 released from $Fe_2(SO_4)_3$ decomposition, the kinetic model proposed by Hindiyarti et al.[13] was adopted in this work. For homogeneous and heterogeneous condensation of K_2SO_4, a first order reaction as used by Li et al. [16] is chosen to describe the processes:

$$K_2SO_4(g) \longrightarrow K_2SO_4(s) \quad (6)$$

The rate constant for the reaction above, $k_{condensation} = 1\times10^{-61}\exp(-150000/T)$ [16], represents the condensation rate predicted from aerosol theory [18].

To simulate the experiments carried out at the VTT grate-reactor, the post-combustion region (port Y1-Y7) of the reactor was modeled as an ideal plug flow reactor. The simulations were carried out with CHEMKIN 4.1.1 [19], using the plug-flow reactor model. The temperature profile used in the simulation was pre-defined (see Figure 3), based on the averaged measured gas temperatures in the different experiments. The amount and composition of the inlet flue gas are estimated based on the experiment without ferric sulfate addition, where the fuel feeding rate is 0.0075 kg/s (wet basis) and the air feeding rate is 0.05 kg/s. The flue gas is assumed to contain only N_2, O_2, CO_2, H_2O, SO_2, HCl, and KCl, with concentrations obtained from the gas analysis or particle measurement.

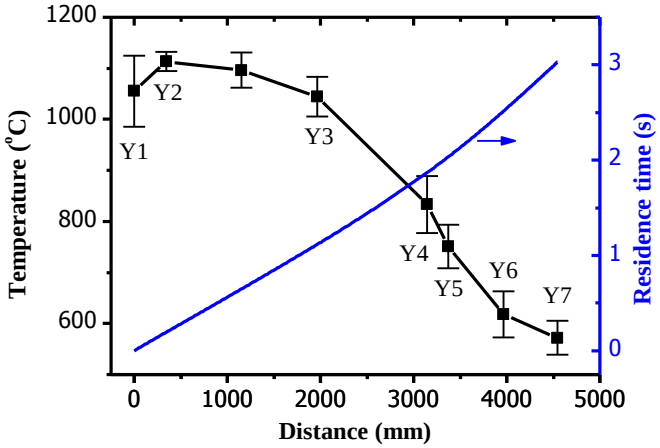

Figure 3 Temperature profile and residence time used in the simulation, from port Y1 to Y7 in Figure 1. The solid symbols represent the average temperatures measured in different experiments, with error bar showing the standard deviation.

4 Results

Figure 4 compares the measured and simulated SO_2 concentrations at port Y7 during different experiments. It can be seen that the concentration of SO_2 are predicted well by the model, both for the experiments with elementary sulfur addition on the grate and for the experiments with $Fe_2(SO_4)_3$ addition at port Y3 or on the grate. For the experiments with elementary S/ $Fe_2(SO_4)_3$ addition on the grate, the simulation results indicate that the only gaseous sulfur species at port Y7 is SO_2. However, for the experiments with $Fe_2(SO_4)_3$ addition at port Y3, trace amount (about 6 ppmv, dry basis) of SO_3 is predicted at port Y7, when the $S_{reagent}/Cl_{fuel}$ ratio becomes 0.6. When the S/Cl ratio is increased to 1.0, the level of SO_3 at port Y7 is predicted to be ~36 ppmv. The results

indicate that when the $Fe_2(SO_4)_3$ is injected at port Y3, an increase of S/Cl ratio from 0.6 to 1.0 may greatly promote the formation of sulfuric acid aerosols, which is qualitatively in agreement with chemical analysis of the collected sub-micron particles in the experiments [5].

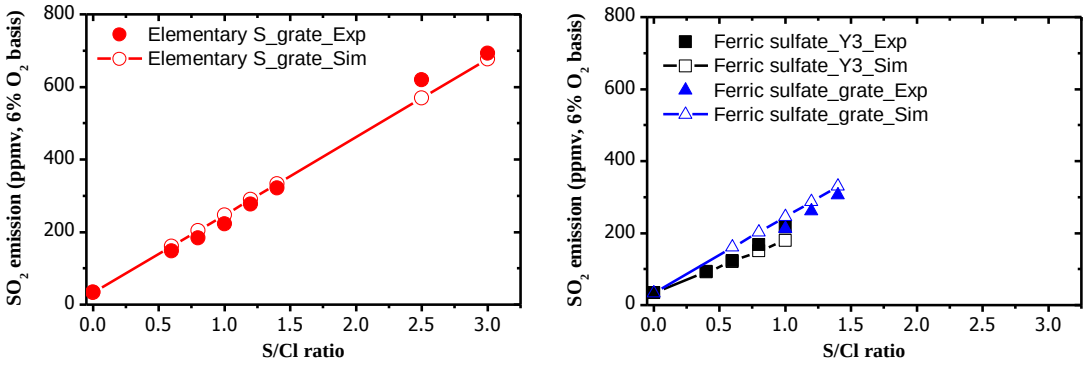

Figure 4 Simulated and measured SO_2 emissions (ppmv, 6% O_2 basis) in the dry flue gas of the VTT grate-firing experiments under different conditions.

In order to quantitatively describe the degree of sulfation in the experiments, the following parameter is introduced:

$$Degree\,of\ sulfation = 1 - \frac{Cl}{K + Na} \tag{9}$$

where the *Cl*, *K* and *Na* are the relevant concentrations (mol%) in the aerosols collected at port Y5.

This degree of sulfation described above is based on the assumption that the alkali metal found in the fine particles is comprised only of sulfates and chlorides. This assumption is believed to be reasonable for the biomass mixture used in this study, as the molar ratio of (K+Na)/(Cl+2S) is approximately 1 in the submicron aerosols collected from the experiments without additives. With this assumption, if all of alkalis in the aerosols are present as alkali chlorides, the calculated sulfation degree would be zero. On the other hand, if the aerosols only contain alkali sulfates, the calculated sulfation degree would be one. During the calculation of the sulfation degree in the experiments, only the aerosol particles in the size range of 0.03-0.62 µm (in a few cases also the range of 0.03-0.26 µm) are considered in Eq. 9, since the majority of the alkali chlorides and sulfates are found in this size range [5]. Therefore it is believed that the sulfation degree calculated from the aerosols in this range is representative. In the simulation, the degree of sulfation is calculated by assuming that all of the KCl, K_2Cl_2, K_2SO_4 and $KHSO_4$ found at port Y5 will end up as aerosols. Therefore the relative concentrations of these species in the flue gas at port Y5 are used to calculate the sulfation degree in the simulation. Sodium is neglected in the simulation due to its small content in the fuel.

The experimental and simulated degrees of sulfation are shown in Figure 5. For the experiments with S-addition, the experimental and simulation results are in good agreement, although the sulfation degree is slightly over-predicted by the simulation. For the experiments with ferric sulfate addition at port Y3, the simulation results compare favorably with the experimental results. However, for the experiments with $Fe_2(SO_4)_3$ addition on the grate, the simulation appears to over-predict the sulfation

degree considerably. A possible explanation is that the simulation only considers the region from port Y1 to port Y7. The high-temperature region from the grate to port Y1 is neglected in the simulation, which may underestimate the conversion from SO_3 to SO_2, thus resulting in an over-prediction of sulfation degree.

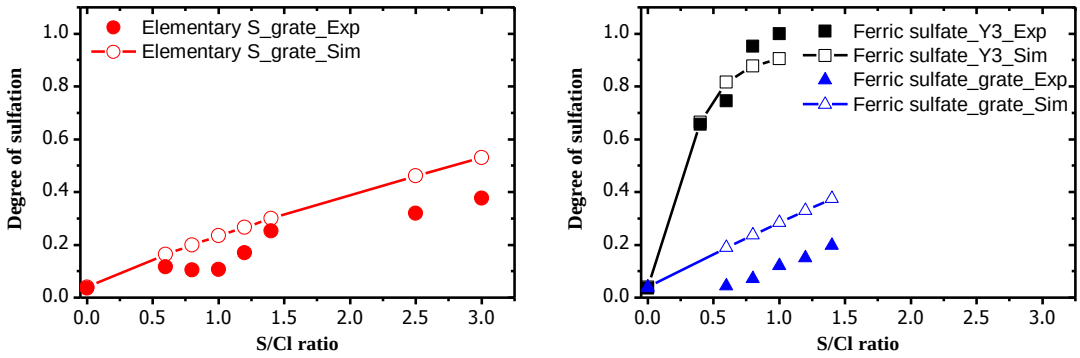

Figure 5 Simulated and measured degree of sulfation at port Y5 during the VVT grate-firing experiments.

The experimental and simulation results shown in Figure 5 imply that $Fe_2(SO_4)_3$ is highly effective when it is injected via port Y3, in a small scale reactor like this. However, when the $Fe_2(SO_4)_3$ is added on the grate, its effectiveness on sulfation of alkali chlorides is almost as low as that of elementary sulfur. In order to explain the different effectiveness obtained with the two injection locations, the concentration profiles of the major sulfur and chlorine species along the reactor are extracted from the simulations. Figure 6a and Figure 6b illustrate the concentration profiles obtained from the simulation of $Fe_2(SO_4)_3$ addition (with $S_{reagent}/Cl_{fuel}$ ratio of 1.0) on the grate and at port Y3, respectively. It can be see that when the $Fe_2(SO_4)_3$ (denoted as SO_3*) is added on the grate, the released SO_3 is largely converted to SO_2 in the high-temperature zone (>1050^{o}C) of port Y1–Y3. The formation of $KHSO_4/K_2SO_4$ is negligible as the reactions are not thermodynamically favorable in this high-temperature zone. However, when the $Fe_2(SO_4)_3$ is injected via port Y3, a considerable fraction of the released SO_3 is contributed to the formation of $KHSO_4$ or K_2SO_4. This is partly because the formation of $KHSO_4/K_2SO_4$ becomes thermodynamically feasible in the zone of port Y3-Y5, where the temperatures are decreased from 1050^{o}C to 750^{o}C. On the other hand, the conversion from SO_3 to SO_2 is less significant between port Y3 and port Y5, due to the relatively low temperatures.

The results of Figure 6 indicate that the effectiveness of $Fe_2(SO_4)_3$ addition on the destruction of KCl is very sensitive to the applied temperature range. It is not favorable to inject $Fe_2(SO_4)_3$ at high temperatures (e.g. above 1050^{o}C), since the majority of the produced SO_3 can be converted rapidly to SO_2. On the other hand, if the ferric sulfate is injected at very low temperatures (e.g. below 800^{o}C), the residence time may not allow a complete decomposition of the additive, thus also affecting its effectiveness. The intermediate temperature range (e.g. between 1050 and 800^{o}C) is more favorable for the injection of $Fe_2(SO_4)_3$. In principle, when the detailed temperature profile in a boiler is known, the model developed in this work can be used to optimize the injection of $Fe_2(SO_4)_3$. In addition, the model can be applied to assess the level of KCl at different boiler locations during $Fe_2(SO_4)_3$ injection. This knowledge may be helpful in order to evaluate the deposition and corrosion risks in the boiler.

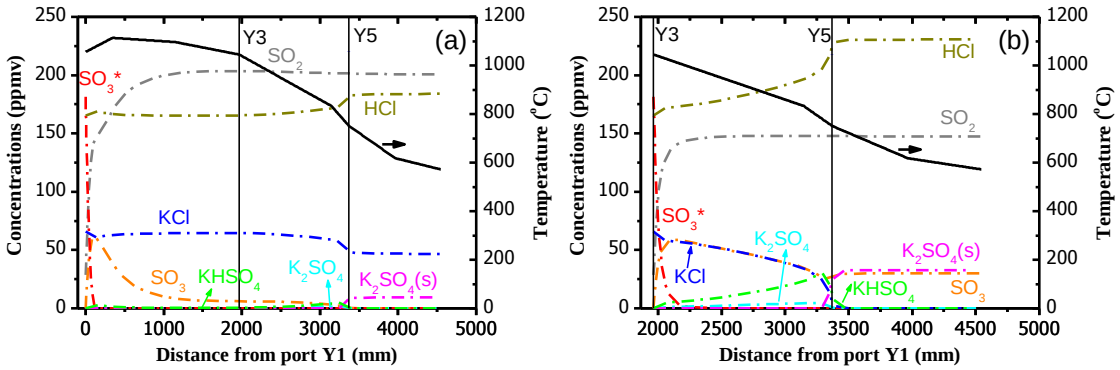

Figure 6 Temperature profile and concentration profiles of the major sulfur and chlorine species during the simulation: (a) ferric sulfate addition on the grate with a $S_{reagent}/Cl_{fuel}$ ratio of 1.0; (b) ferric sulfate addition at port Y3 with a $S_{reagent}/Cl_{fuel}$ ratio of 1.0. SO_3* represents the injected ferric sulfate; K_2SO_4(s) denotes the potassium sulfate aerosols; KCl contains both potassium chloride and its dimmer; Y5 denotes the aerosol sampling point in the experiments.

5 Conclusions

Decomposition of $Fe_2(SO_4)_3$ is studied in a high-heating rate TGA and a laboratory-scale tube-reactor. The TGA experiments reveal that the decomposition of $Fe_2(SO_4)_3$ can be described well by a volumetric reaction model with kinetic parameters derived from the experiments under isothermal conditions. The experiments in the tube-reactor imply that the sulfur released from ferric sulfate decomposition is distributed as approximately 40% SO_3 and 60% SO_2 in the temperature range of 700–1000 ^oC.

Based on the obtained kinetic parameters and the distribution of sulfur products, a model is proposed to describe the decomposition of $Fe_2(SO_4)_3$ under the conditions of a grate-firing reactor. By combining the ferric sulfate decomposition model with a detailed gas phase kinetic model of KCl sulfation [13] and a simplified model of K_2SO_4 condensation [16], the sulfation of KCl by $Fe_2(SO_4)_3$ addition during grate-firing of biomass is simulated. The simulation results compare favorably with the experimental results obtained in a pilot-scale biomass grate-firing reactor where different amount of $Fe_2(SO_4)_3$ was injected on the grate or into the free-board [5]. The simulation results suggest that the SO_3 released from ferric sulfate decomposition is the main contributor to KCl sulfation. The effectiveness of $Fe_2(SO_4)_3$ addition towards KCl destruction is sensitive to the applied temperature range. For a boiler with known temperature profile and KCl level, the model developed in this work would be helpful in order to optimize the injection of ferric sulfate and to minimize deposition and corrosion risks.

6 Acknowledgements

Funding from EU contract 23946 “Demonstration of a 16 MW high energy efficient corn stover biomass power plant” was gratefully acknowledged.

REFERENCES

[1] H. Kassman, L. Bäfver, L.E. Åmand, The importance of SO2 and SO3 for sulphation of gaseous KCl-An experimental investigation in a biomass fired CFB boiler, Combust. Flame. 157 (2010) 1649-1657.

[2] K.O. Davidsson, L.E. Åmand, B.M. Steenari, A.L. Elled, D. Eskilsson, B. Leckner, Countermeasures against alkali-related problems during combustion of biomass in a circulating fluidized bed boiler, Chemical Engineering Science. 63 (2008) 5314-5329.
[3] Y. Zheng, P.A. Jensen, A.D. Jensen, B. Sander, H. Junker, Ash transformation during co-firing coal and straw, Fuel. 86 (2007) 1008-1020.
[4] K. Iisa, Y. Lu, K. Salmenoja, Sulfation of potassium chloride at combustion conditions, Energy Fuels. 13 (1999) 1184-1190.
[5] M. Aho, K. Paakkinen, R. Taipale, Destruction of alkali chlorides using sulphur and ferric sulphate during grate combustion of corn stover and wood chip blends, Fuel. 103 (2013) 562-569.
[6] H. Wu, P. Glarborg, F.J. Frandsen, K. Dam-Johansen, P.A. Jensen, B. Sander, Trace elements in co-combustion of solid recovered fuel and coal, Fuel Process. Technol. 105 (2013) 212-221.
[7] H. Kassman, M. Broström, M. Berg, L.E. Åmand, Measures to reduce chlorine in deposits: Application in a large-scale circulating fluidised bed boiler firing biomass, Fuel. 90 (2011) 1325-1334.
[8] J.H. Zeuthen, P.A. Jensen, J.P. Jensen, H. Livbjerg, Aerosol formation during the combustion of straw with addition of sorbents, Energy Fuels. 21 (2007) 699-709.
[9] H. Wu, P. Glarborg, F.J. Frandsen, K. Dam-Johansen, P.A. Jensen, B. Sander, Co-combustion of pulverized coal and solid recovered fuel in an entrained flow reactor – General combustion and ash behaviour, Fuel. 90 (2011) 1980-1991.
[10] M. Broström, H. Kassman, A. Helgesson, M. Berg, C. Andersson, R. Backman, et al., Sulfation of corrosive alkali chlorides by ammonium sulfate in a biomass fired CFB boiler, Fuel Process. Technol. 88 (2007) 1171-1177.
[11] M. Aho, P. Vainikka, R. Taipale, P. Yrjas, Effective new chemicals to prevent corrosion due to chlorine in power plant superheaters, Fuel. 87 (2008) 647-654.
[12] P. Glarborg, P. Marshall, Mechanism and modeling of the formation of gaseous alkali sulfates, Combust. Flame. 141 (2005) 22-39.
[13] L. Hindiyarti, F. Frandsen, H. Livbjerg, P. Glarborg, P. Marshall, An exploratory study of alkali sulfate aerosol formation during biomass combustion, Fuel. 87 (2008) 1591-1600.
[14] T.L. Jørgensen, H. Livbjerg, P. Glarborg, Homogeneous and heterogeneously catalyzed oxidation of SO2, Chem. Eng. Sci. 62 (2007) 4496-4499.
[15] H. Kassman, J. Pettersson, B.M. Steenari, L.E. Åmand, Two strategies to reduce gaseous KCl and chlorine in deposits during biomass combustion—injection of ammonium sulphate and co-combustion with peat, Fuel Process Technol. (2011).
[16] B. Li, Z. Sun, Z. Li, M. Aldén, J.G. Jakobsen, S. Hansen, et al., Post-flame gas-phase sulfation of potassium chloride, Combust. Flame. 160 (2013) 959-969.
[17] M. Aho, K. Paakkinen, R. Taipale, Quality of deposits during grate combustion of corn stover and wood chip blends, Fuel. 104 (2013) 476-487.
[18] K.A. Christensen, H. Livbjerg, A plug flow model for chemical reactions and aerosol nucleation and growth in an alkali-containing flue gas, Aerosol Sci. Tech. 33 (2000) 470-489.
[19] R. Kee, F. Rupley, J. Miller, M. Coltrin, J. Grcar, E. Meeks, et al., CHEMKIN, release 4.1. 1; Reaction Design: San Diego, CA, 2007,.